

Hemilabile Ligand Induced Selectivity: a DFT Study on Ethylene Trimerization Catalyzed by Titanium Complexes

Theodorus J. M. de Bruin,[†] Lionel Magna,[‡] Pascal Raybaud,^{*,†} and Hervé Toulhoat[§]

Division Chimie et Physico-Chimie Appliquées, Département Thermodynamique et Modélisation Moléculaire, Division Catalyse et Séparation, Département Catalyse Moléculaire, and Direction Scientifique, Institut Français du Pétrole, 1-4 Avenue de Bois Préau, 92852 Rueil-Malmaison Cedex, France

Received April 7, 2003

In this computational study, we propose a detailed mechanism, which has been explored by density functional theory simulations, for the trimerization reaction of ethylene to give selectively 1-hexene using a $[(\eta^5\text{-C}_5\text{H}_4\text{CMe}_2\text{C}_6\text{H}_5)\text{TiCl}_3/\text{MAO}]$ catalyst. For ring-opening reactions we distinguish between agostic assisted β -hydrogen transfer and hydride formation. With the B3LYP functional it was found that the rate-determining step is the ring-opening reaction of the seven-membered metallacycle, exhibiting a barrier $\Delta G^\ddagger(298.15\text{ K})$ of 18.4 kcal/mol. It appears that the selectivity of the reaction results from two effects: the stabilizing effect of the hemilabile phenyl ligand and the ring size of the metallacycle. Upon interchange of the phenyl group by the labile methyl group, the calculations predict the formation of polyethylene, which is in agreement with the experimental data.

1. Introduction

The production process of α -olefins forms an important domain in petrochemistry. There is a growing demand for light α -olefins, and indeed, linear α -olefins are being used more and more as comonomers¹ in catalytic olefin polymerization for the production of different linear low-density polyethylene grades.² In this context there is a strong incentive for the selective trimerization of ethylene to 1-hexene.

Recently, Hessen and co-workers published a highly selective method to produce 1-hexene with the use of a titanium complex with a hemilabile ancillary ligand ($\eta^5\text{-C}_5\text{H}_4\text{CMe}_2\text{R}$) and methylalumoxane (MAO) as cocatalyst (Scheme 1).³ In their study, they found that hemilabile ligands with R = phenyl, 3,5-dimethylphenyl show a large selectivity toward 1-hexene, whereas a ligand with R = methyl leads to polyethylene. In addition, a significant decrease in activity was observed upon going from R = phenyl to R = 3,5-dimethylphenyl to R = methyl. The authors have proposed a reaction pathway for the catalyst transformation and catalytic trimerization of ethylene, involving metallacycle intermediates.⁴

In the present work we will investigate this mechanism in detail by ab initio techniques.

Computational chemistry, and in particular density functional theory, has been proven to give relevant insights and has contributed to a better understanding of the reaction mechanisms that play a role in homogeneous catalysis.⁵ A large number of the transition-metal elements that show catalytic activity in homogeneous catalysis for the polymerization of ethylene has already been subjected to a computational analysis.⁶ However, oligomerization processes involving metallacycles have, up to now, received considerably less attention, despite their high selectivity and promising future. Only very recently, Yu and Houk⁷ computationally explored the trimerization process based on a tantalum system that was developed by Sen and co-workers.⁸ However, in this system there is no pending ligand present, which plays a major role in the final selectivity of the reaction in the titanium catalytic system.

In the present paper, we investigate the oligomerization reaction using the titanium complex in detail by

* To whom correspondence should be addressed. E-mail: pascal.raybaud@ifp.fr. Tel: +33 (0)1.47.52.71.84. Fax: +33 (0)1.47.52.70.58.

[†] Division Chimie et Physico-Chimie Appliquées, Département Thermodynamique et Modélisation Moléculaire.

[‡] Division Catalyse et Séparation, Département Catalyse Moléculaire.

[§] Direction Scientifique.

(1) Tait, P. J. T.; Berry, I. G. *Comprehensive Polymer Science*; Eastmond, G. C., Ledwith, A., Russo, S., Sigwalt, P., Eds.; Pergamon Press: Oxford, U.K., 1989; Vol. 4, p 575.

(2) Hennico, A.; Leonard, J.; Forestiere, A.; Glaize, Y. *Hydrocarbon Process.* **1990**, *69*, 73.

(3) (a) Deckers, P. J. W.; Hessen, B.; Teuben, J. H. *Angew. Chem., Int. Ed.* **2001**, *40*, 2516–2519. (b) Deckers, P. J. W.; Hessen, B.; Teuben, J. H. *Organometallics* **2002**, *21*, 5122–5135.

(4) Briggs, J. R. *J. Chem. Soc., Chem. Commun.* **1989**, 674–675.

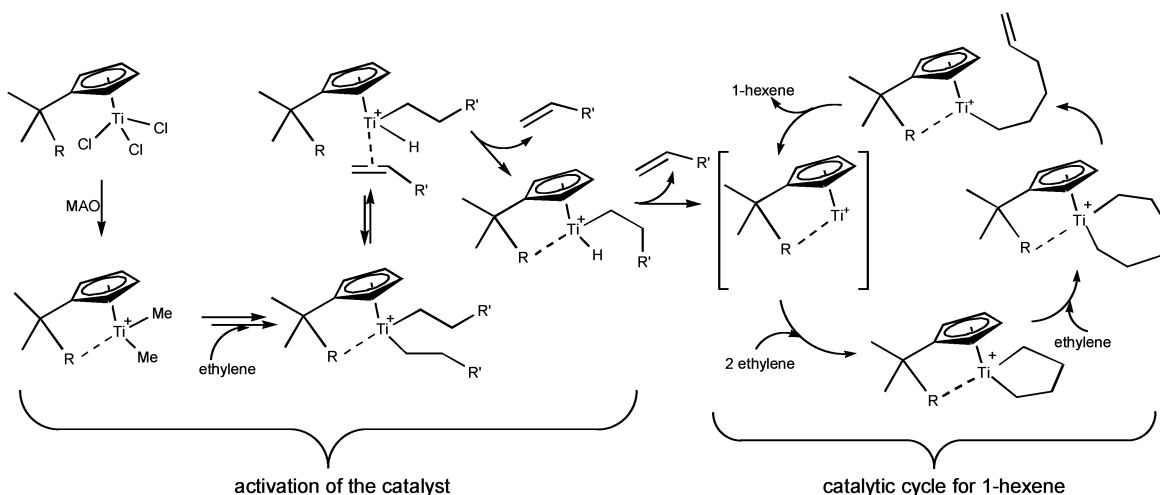
(5) (a) Niu, S.; Hall, M. B. *Chem. Rev.* **2000**, *100*, 353–405. (b) Yoshida, Y.; Matsui, S.; Takagi, Y.; Mitani, M.; Nakano, T.; Tanaka, H.; Kashiwa, N.; Fujita, T. *Organometallics* **2001**, *20*, 4793–4799.

(6) (a) Jensen, V. R.; Angermund, K.; Jolly, P. W.; Børve, K. J. *Organometallics* **2000**, *19*, 403–410. (b) Döhring, A.; Jensen, V. R.; Jolly, P. W.; Thiel, W.; Weber, J. C. *Organometallics* **2001**, *20*, 2234–2245. (c) Derat, E.; Bouquant, J.; Bertus, P.; Szymoniak, J.; Humbel, S. J. *Organomet. Chem.* **2002**, *664*, 268–276. (d) Chan, M. S. W.; Deng, L.; Ziegler, T. *Organometallics* **2000**, *19*, 2741–2750. (e) Chan, M. S. W.; Ziegler, T. *Organometallics* **2000**, *19*, 5182–5189. (f) Vanka, K.; Ziegler, T. *Organometallics* **2001**, *20*, 905–913.

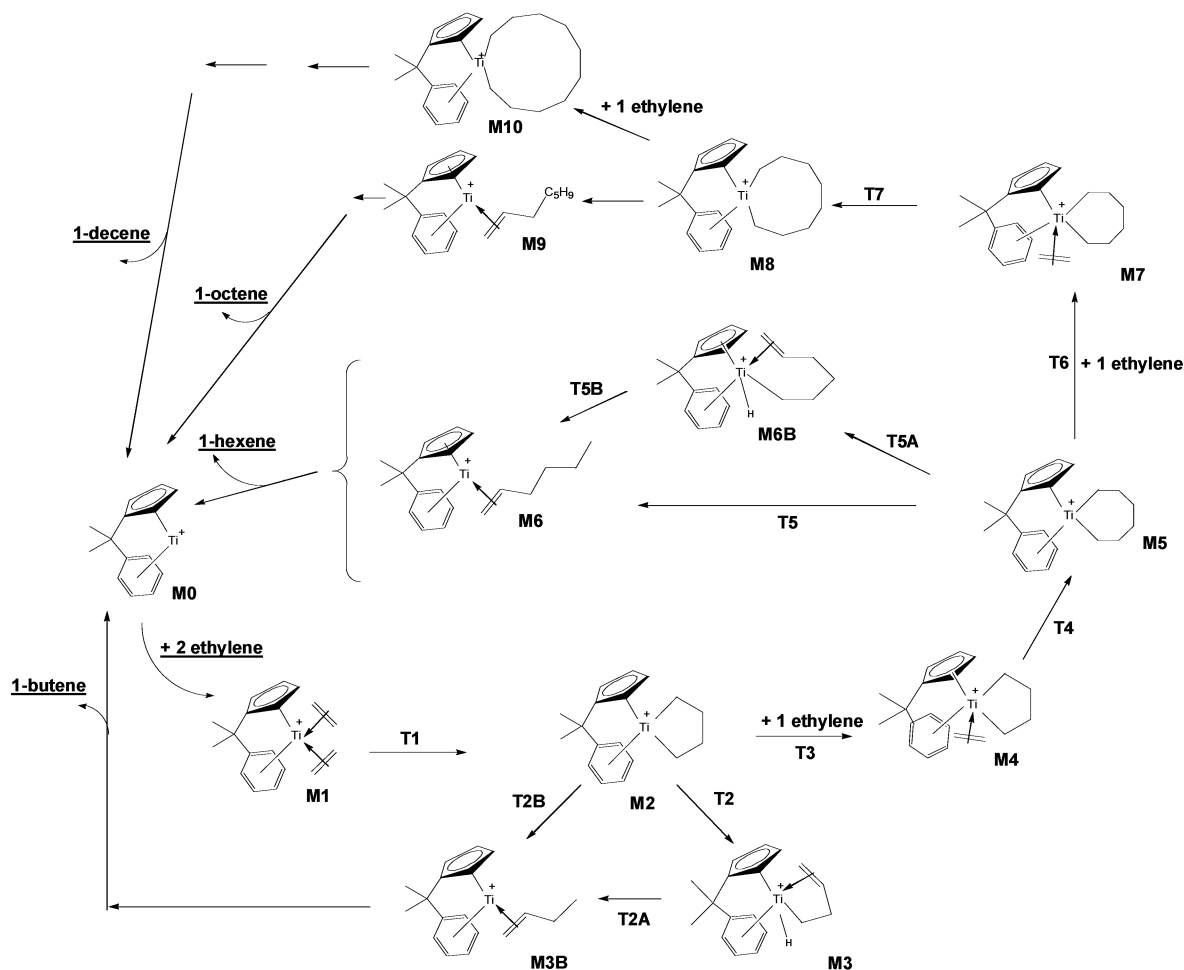
(7) Yu, Z.-X.; Houk, K. N. *Angew. Chem., Int. Ed.* **2003**, *42*, 808–810.

(8) Andes, C.; Harkins, S. B.; Murtoza, S.; Oyler, K.; Sen, A. *J. Am. Chem. Soc.* **2001**, *123*, 7423.

Scheme 1



Scheme 2



applying density functional theory to bring new insights that could assist in elucidating the essential steps that are responsible for the observed high selectivity, which in return could help to improve development of better catalysts. For that purpose, we propose the mechanism given in Scheme 2, for which all stationary points have been located on the B3LYP/LACVP (see Theoretical Methods) surface. The mechanistic steps for the activation of the catalyst precursor with the MAO cocatalyst have deliberately been omitted in this scheme, since we

want to study the influence of the hemilabile R group in the catalytic cycle only.

Compound **M0** is our starting structure, in which the titanium has the oxidation state II. This highly unsaturated, and therefore probably "virtual", species will immediately accept the coordination of two ethylene molecules (**M1**), from which a five-membered metallocycle is formed (**M2**); meanwhile the Ti(II) is oxidized to Ti(IV). Subsequently, a ring-opening reaction can occur to yield 1-butene, via two different mechanisms.

Either there is a β -hydrogen transfer to the Ti (**M3**) followed by a reductive elimination or there can be a direct agostic assisted intramolecular β -hydrogen transfer (**M3B**), in which the Ti(IV)⁺ ion is directly reduced to Ti(II)⁺ and the olefin is only bonded to the Ti via a Ti– π interaction. However, given that experimentally no 1-butene is observed, the reaction is thought to be continued to obtain **M4**, in which a third ethylene molecule has been coordinated. After ethylene insertion (**M5**), the reaction might continue with a ring opening (**M6** and **M6B**) to finally produce 1-hexene (experimentally observed). Theoretically, the reaction may also proceed with the insertion of a new ethylene molecule to give **M7**, which leads to 1-octene or even larger α -unsaturated olefins via **M10** to produce 1-decene etc. Although these latter species are not experimentally found, this result should also follow from our calculations.

In this theoretical study, we will explore the trimerization reaction of ethylene by applying the B3LYP functional to Scheme 2, to find a theoretical explanation for the observed experimental selectivity and to gain insights into the mechanism of ring-opening reactions.

2. Theoretical Methods

All geometry optimizations were performed with the Jaguar suite of programs⁹ and the unrestricted B3LYP functional¹⁰ with the use of the LACVP basis set: i.e., LANL2DZ for Ti¹¹ and 6-31G(d,p) for C and H, referred to after this point as BS1. All structure optimizations were performed without any geometrical constraints, except for **T3** and **T6**, which correspond to the transition-state structures for the coordination of an ethylene molecule. These two transition states were located by minimizing all degrees of freedom, while keeping the reaction coordinate (i.e., one of the two Ti–C_{ethylene} distances) fixed. All stationary points were subjected to a frequency analysis to verify the desired state of the stationary point (minimum or transition state) and to include the Gibbs free energy corrections. These frequency calculations were performed with the Gaussian 98 package of programs at the same level of theory.¹²

Additionally, the electronic configuration was considered for **M0**, which is the poorest electron species with respect to the 18-electron rule. It was found that at the B3LYP/BS1 level the singlet state is considerably more stable than the triplet state (5.3 kcal/mol); for **M5**, chosen as a representative “saturated” compound, this difference even increases up to 51.9 kcal/mol. From these results the assumption was made that all other species in Scheme 2 are likely to exhibit a singlet electronic configuration.

To have a more precise notion of the energy barriers, single-point energies were calculated for all stationary points at the

B3LYP level with an improved basis set: cc-pVTZ (without f functions) and a triple- ζ contraction of the Hay–Wadt pseudo-potential, henceforth referred to as BS2.¹³ For the final energy evaluation the SCF energy was used from BS2 together with the Gibbs free energy corrections calculated with BS1. All energies (in kcal/mol) are referenced to the total energy of **M0** plus the corresponding number of ethylene molecules. For the calculations performed with Jaguar, the pseudospectral method was used to speed up the calculations. It has been verified that the application of this method does not significantly change the accuracy of the energy differences.¹⁴

Natural population analyses (NPA charges) were obtained from the Gaussian NBO program¹⁵ at the B3LYP/BS1 level.

3. Results and Discussion

Geometrical Aspects. Structure **M0**, which lacks two ligands, is highly unsaturated. The negatively charged cyclopentadienyl ligand (Cp) and the phenyl group are both firmly bound to the Ti⁺ ion. These ligands are bonded to the Ti⁺ in η^5 and η^6 modes, respectively. Both ligands have their shortest Ti–C bond for the carbon atom directly connected to the methylene bridge (2.22 and 2.18 Å), whereas the carbon atoms at the meta positions of the phenyl and at the 3,4-positions of the Cp have the longest Ti–C bond lengths: \sim 2.40 and 2.36 Å, respectively. The nearly equal average Ti–C_{phenyl} and Ti–C_{Cp} distances indicate that both ligands are equally well bound, despite the additional electrostatic interaction between the negatively charged Cp ring and the positively charged Ti center. Furthermore, it should be noted that the phenyl ring is no longer completely flat and thus has partly lost its aromatic character. **M0** is a formal 14-electron species and lacks 4 electrons to fulfill the 18-valence-electron rule. This species is therefore willing to accept the coordination of electron-donating ligands, such as an ethylene molecule. Upon additions of two ethylene molecules the binding mode of the phenyl ring drastically changes. The shortest Ti–C distance becomes 2.40 Å, and the average distance increases from 2.34 to 3.46 Å. This already reveals the hemilabile character of the phenyl group. The Cp group remains bonded to the Ti center. The coordinated ethylene molecules have a strong interaction with the Ti, as can be seen from the Ti–C distances 2.25 and 2.39 Å (ethylene 1) and 2.27 and 2.43 Å (ethylene 2). The elongated C–C bond distance in the coordinated ethylene molecule (1.39 Å vs 1.33 Å noncoordinated) clearly indicates that there is a substantial amount of electron back-donation of the filled d orbitals into the empty π^* orbital of the ethylene. Both ethylene molecules are coordinated in such a way that they form, with the Ti center, almost a flat plane.¹⁶ The adopted positions of the ethylene molecules are adequate to form the new C–C σ -bond. In the transition structure **T1** this bond is 2.03 Å and the two new Ti–C σ -bonds are 2.10 and 2.11 Å (Figure 1).¹⁷ Once the metallacycle reaction has completed, **M2**, these latter

(9) Jaguar 4.2; Schrödinger, LLC, Portland, OR, 1991–2002.

(10) (a) Becke, A. D. *J. Chem. Phys.* **1993**, *98*, 5648–5652. (b) Lee, C.; Yang, W.; Parr, R. G. *Phys. Rev. B* **1988**, *37*, 785–789.

(11) Hay, P. J.; Wadt, W. R. *J. Chem. Phys.* **1985**, *82*, 299–310.

(12) Frisch, M. J.; Trucks, G. W.; Schlegel, H. B.; Scuseria, G. E.; Robb, M. A.; Cheeseman, J. R.; Zakrzewski, V. G.; Montgomery, J. A., Jr.; Stratmann, R. E.; Burant, J. C.; Dapprich, S.; Millam, J. M.; Daniels, A. D.; Kudin, K. N.; Strain, M. C.; Farkas, O.; Tomasi, J.; Barone, V.; Cossi, M.; Cammi, R.; Mennucci, B.; Pomelli, C.; Adamo, C.; Clifford, S.; Ochterski, J.; Petersson, G. A.; Ayala, P. Y.; Cui, Q.; Morokuma, K.; Malick, D. K.; Rabuck, A. D.; Raghavachari, K.; Foresman, J. B.; Cioslowski, J.; Ortiz, J. V.; Stefanov, B. B.; Liu, G.; Liashenko, A.; Piskorz, P.; Komaromi, I.; Gomperts, R.; Martin, R. L.; Fox, D. J.; Keith, T.; Al-Laham, M. A.; Peng, C. Y.; Nanayakkara, A.; Gonzalez, C.; Challacombe, M.; Gill, P. M. W.; Johnson, B. G.; Chen, W.; Wong, M. W.; Andres, J. L.; Head-Gordon, M.; Replogle, E. S.; Pople, J. A. *Gaussian 98*, revision A.7; Gaussian, Inc.: Pittsburgh, PA, 1998.

(13) These single-point calculations were performed with the Jaguar suite of programs.⁹

(14) The difference between the SCF energies of **M5** and **T5** with and without the pseudospectral method using BS2 is <0.09 kcal/mol.

(15) Glendening, E. D.; Reed, A. E.; Carpenter, J. E.; Weinhold, F. *Gaussian NBO program*, version 3.1.

(16) There also exists another minimum in which the two ethylene molecules are perpendicular with respect to each other, but this minimum has a higher energy.

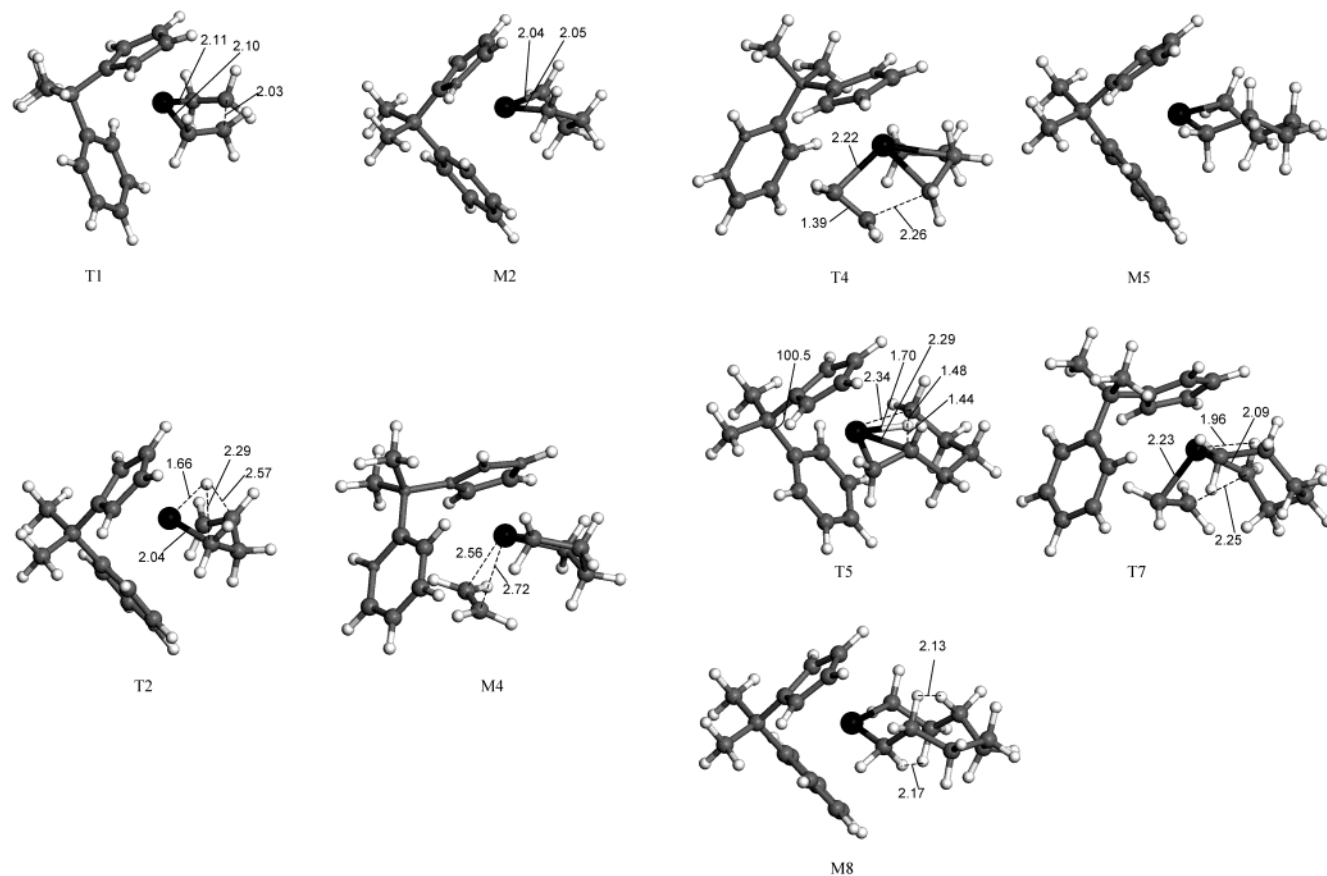
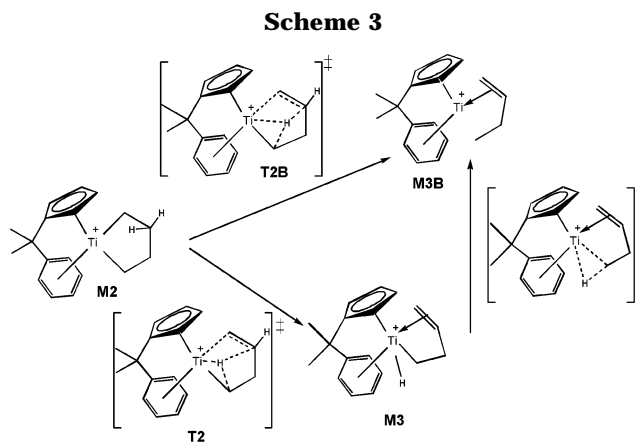


Figure 1. Select number of optimized geometries, minima, and transition-state structures, on the B3LYP/BS1 surface with some relevant geometrical features. All distances are in Å and bond angles in degrees. The titanium atom is displayed in black, carbon atoms in gray, and hydrogen atoms in white.

distances relax to 2.04 and 2.05 Å, respectively; the C–C σ -bond becomes 1.55 Å. The average Ti–C_{phenyl} distance varies along the steps **M1** → **T1** → **M2** only from 3.46 to 3.42 Å, respectively. This reveals that the phenyl group does not play a major role during the formation of the metallacycle. Additionally, it can be mentioned that during this reaction step (coordination of two ethylene molecules), the oxidation state of the Ti changes from II to IV.

Once the metallacycle **M2** has been formed, the reaction can proceed by either the coordination of a new ethylene molecule or a ring-opening reaction. The opening can take place in two different ways (Scheme 3). The first pathway involves a β -hydrogen transfer to the Ti center, while the oxidation state of Ti remains unchanged (**M3**), and 1-butene is coordinated to Ti at the 4-position involving a σ -bond. This reaction step is subsequently followed by a reductive elimination reaction to finally yield **M3B**. This reductive elimination has been proposed for Cr and Pt systems.¹⁸ In the second proposed pathway, the reduction of the Ti center occurs immediately due to an agostic β -hydrogen transfer, now yielding 1-butene that is coordinated to Ti via a π -bond (**M3B**). To our knowledge, no clear evidence is available in the literature that indicates which pathway is the



preferred one for ring-opening reactions involving Ti. Our calculations show that, for a relatively small metallacycle as **M2**, the ring opening seems to occur exclusively via the first pathway involving the Ti–H species. This behavior has also been observed by Yu and Houk on an analogous TaCl₃ system, in which the ring-opening reaction of the five-membered ring also occurred in a two-step way, instead of the concerted reductive elimination.

It has explicitly been verified that **T2** indeed connects **M2** and **M3** by an intrinsic reaction coordinate calculation. The size of the metallacycle appears to hamper the second ring-opening reaction type, since **T2B** could not be located on the potential energy surface (PES) (vide

(17) Structures **M1** and **T1** resemble to some extent the structures **2** and **TS1** in the paper of Wu and Yu (Wu, Y.-D.; Yu, Z.-X. *J. Am. Chem. Soc.* **2001**, *123*, 5777–5786). In the transition-state structure, the distance between the two carbon–carbon atoms forming a σ bond is 2.088 Å.

(18) McDermott, J. X.; White, J. F.; Whitesides, G. M. *J. Am. Chem. Soc.* **1973**, *95*, 4451–4452.

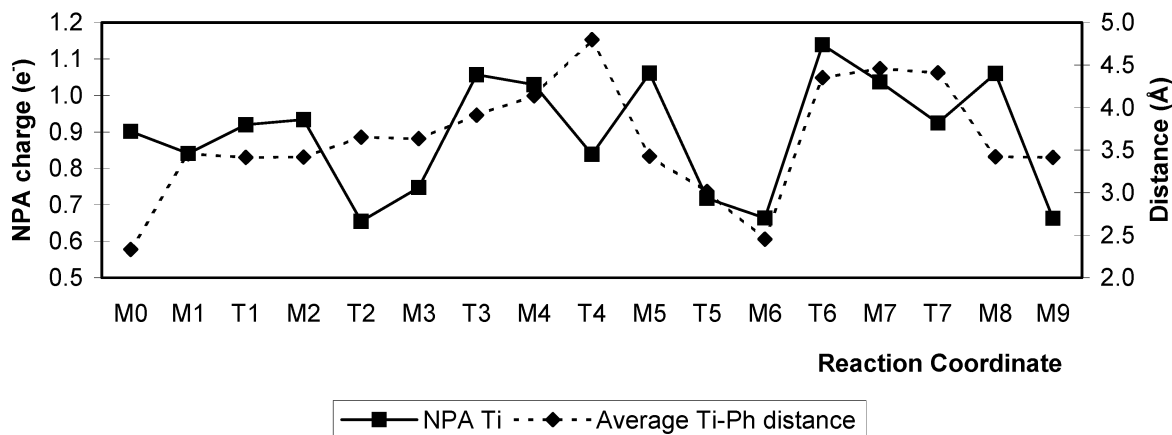


Figure 2. Atomic charge on Ti calculated using the natural population analysis scheme and the average Ti–C_{phenyl} distance as a function of the reaction coordinate. Note that the lines connecting the data points have no physical meaning.

infra). In addition, the phenyl ligand remains coordinated to the Ti center during the ring-opening reaction.

The coordination of an additional (third) ethylene molecule causes, for the first time, a complete dissociation of the phenyl ligand from the metal center: the shortest Ti–C distance is 3.28 Å, and the average distance is 4.14 Å. It may be noted that for **M4** two starting structures have been used, one with a strong Ti–phenyl interaction and one in which the phenyl was already dissociated. Both geometries essentially lead to the same final optimized structure (**M4**). The Ti–ethylene interaction is significantly less strong in **M4** as compared to that in **M1**, as can be seen from the considerably longer bond lengths $r(\text{Ti}-\text{C}_{\text{ethylene}}) = 2.56$ and 2.72 Å (Figure 1). During the insertion step of the third ethylene (**T4**), the phenyl is still completely dissociated ($\text{Ti}-\text{C}_{\text{phenyl}}(\text{average}) = 4.80$ Å) and, once the insertion step has completed (**M5**), the phenyl takes up an orientation similar to that in **M2** with $\text{Ti}-\text{C}_{\text{phenyl}}(\text{average}) = 3.43$ Å. In the transition-state geometry **T4**, the inserted C–C bond is 2.26 Å; the ethylene carbon atom that is undergoing the insertion has $r(\text{Ti}-\text{C}) = 2.51$ Å, and the other ethylene carbon has $r(\text{Ti}-\text{C}) = 2.22$ Å. The new C–C bond is 1.54 Å, and the new σ Ti–C bond is 2.06 Å in **M5**. It is noteworthy to mention that during the insertion processes, the metallacycle becomes deformed, i.e., its radius becomes smaller, due to the loss of the σ Ti–C bond and the creation of two π bonds (see Figure 1, **T4**). Since the ethylene molecule being inserted is slightly pushed away as a result of the smaller metallacycle, it also prevents the phenyl group from coordinating to the Ti center.

Since **M5** is the “higher” homologue of **M2**, again, either a ring-opening reaction can occur or the reaction can proceed by taking up a new (fourth) ethylene molecule. We will first discuss the two possible ring-opening reactions. In contrast to **M2**, ring opening of **M5** primary takes place via a direct hydrogen transfer in the hydrocarbon cycle, assisted by the Ti metal center (**T5**). No stationary point on the PES could be located for the analogue of **T2**, i.e., **T5A** (vide infra).

The transition state **T5** is stabilized by the phenyl ring, indicated by a relatively short average Ti–C_{phenyl} distance (3.01 Å). This distance is significantly shorter in **T5** than in **T2**, where it is 3.65 Å. Note that this

increased Ti–phenyl interaction causes some deviation of the ideal bond angle $\text{C}_{\text{phenyl}}-\text{C}(\text{Me})_2-\text{C}_{\text{Cp}}$: 100.5° (Figure 1).

Although both transition states (**T2** and **T5**) resemble each other to some extent, there are some important differences. In **T5**, the hydrogen, the titanium, and the two carbon atoms that are involved in the hydrogen transfer all lie practically in the same plane. Such a geometry is not possible in **T2**, due to the small ring size of the metallacycle. In that case, the hydrogen undergoing the transfer lies “above” the plane formed by Ti and the two carbon atoms, making a kind of tetrahedral configuration (Figure 1). Moreover, the $r(\text{C}-\text{H})$ distances are significantly shorter and practically equidistant in **T5** (1.48 and 1.44 Å), whereas in **T2** the distances are significantly longer (2.04 and 2.57 Å). On the other hand, the distance Ti–H in **T2** is slightly smaller than in **T5**: 1.66 and 1.70 Å, respectively. On the basis of these geometrical features, it can be understood that **T2** first proceeds to **M3** (i.e. the Ti–H species) and then to **M3B**, which is the smaller analogue of **T5**.

Addition of a fourth ethylene molecule yields **M7**. The ethylene coordinates in a way similar to that in **M4**, and also the Ti–C_{ethylene} distances are comparable: 2.54 and 2.77 Å in **M7** and 2.56 and 2.72, respectively, in **M4**. The transition-state structure for the insertion step (**T7**) is very much like **T4**. The distances of the newly formed C–C bond are as follows: 2.25 Å (2.26 in **T4**); Ti–C_{inserted} = 2.49 Å (2.51 in **T4**); Ti–C = 2.23 Å (2.22 in **T4**). The Ti–C bond distance that is to be broken is 2.09 Å. This insertion process appears to be assisted by an additional agostic Ti–H interaction of a hydrogen atom on the methylene group: $r(\text{Ti}-\text{H}) = 1.96$ Å. Such an interaction is absent in **T4**. It is worth mentioning that the C–C bond insertion in **T7** takes place exactly on the other side of the metallacycle as compared to **T4**. On the basis of only geometrical features, it cannot be excluded that species such as **T7**, leading finally to 1-octene, are being formed.

Natural Population Analyses. The evolution of the NPA charge on the Ti center and the average Ti–C_{phenyl} distance are both plotted against the reaction coordinate in Figure 2. As a result of the strong Ti–phenyl interaction in **M0** the NPA charge on the Ti center does not deviate too much from its formal +1 charge: 0.902

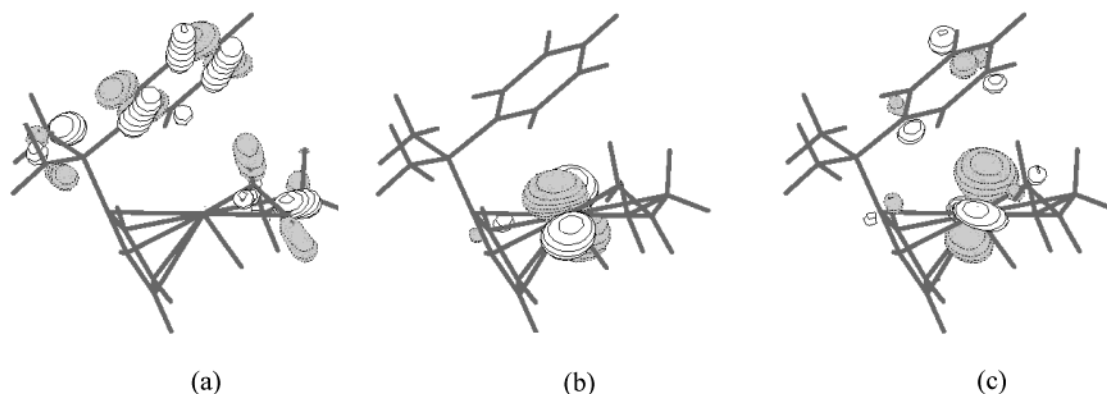


Figure 3. Representation of HOMO-10 (a), LUMO (b), and LUMO+2 (c) of **T2**.

e. Indeed, upon decooordination of the phenyl group in **M0**, the NPA charge increases to 1.167 e. Upon coordination of two ethylene molecules the average Ti–phenyl distance significantly increases, while the NPA only slightly diminishes. In other words, a net electron transfer from the ethylene molecules to the Ti center compensates for the charge increase on the Ti due to the partial decooordination of the phenyl group.

The NPA charge, as well as the average Ti–phenyl distance, remains practically constant for **M1**, **T1**, **M2**, and **M3**. The Ti–H interaction ($r(\text{Ti}-\text{H}) = 1.66 \text{ \AA}$ in **T2**) has a considerable influence on the NPA charge of Ti, since the net atomic charge drops from 0.934 e in **M2** to 0.655 e in **T2**. Since the hydrogen atom coordinates on the opposite side of the plane defined by the Ti center and “1-butene”, there would in principle be sufficient space for the phenyl group to coordinate to the Ti center. However, the average Ti–C_{phenyl} distance remains fairly constant and even shows a small increase across the series **T1** → **M2** → **T2**: 3.42 to 3.42 to 3.65 Å. The decrease in NPA charge on the Ti could partly explain the weakening of the Ti–phenyl interaction, assuming that electrostatic interactions play a role. Additionally, from the molecular orbital (MO) analysis it follows that either the empty d orbitals of Ti which in principle could accept the π electrons of the phenyl group do not have the correct symmetry or the MO has the wrong sign. The lowest unoccupied molecular orbital (LUMO), which has a large d orbital character on the Ti (Figure 3b), has no net overlap with the occupied MO that describes the π orbitals of the phenyl group (level HOMO-10; Figure 3a). The next empty MO that mainly has a d orbital character (level LUMO+2) has an antibonding interaction with the HOMO-10 (Figure 3c).

In the series **M3**, **T3**, **M4**, and **T4** the average Ti–phenyl distances increase as a result of a new ethylene molecule that enters, which forces the phenyl group to decoordinate, resulting in a minor increase of the NPA on Ti. However, in **T4**, in which the ethylene is being inserted into the metallacycle, the NPA charge drops rather drastically, likely due to a Ti–H interaction ($r(\text{Ti}-\text{H}) = 2.23 \text{ \AA}$) in combination with the change in mode of coordination of both the ethylene molecule and the metallacycle itself to the Ti center. Upon going from **T4** to **M5**, **T5**, and **M6**, the phenyl group approaches the Ti center more and more. Intuitively, this would cause a decrease in the NPA charge on the Ti due to the electron flow from the phenyl group to the Ti. Actually, this is the case for **T5** and **M6**, but in those

Table 1. Charge Decomposition Analysis of the Phenyl–Ti Interaction for the Species **T4 and **M5** by Use of the CDA Program**

	T4	M5
donation (e)	0.133	0.421
back-donation (e)	0.015	0.019
repulsive polarization (e)	−0.091	−0.139
residual (e)	−0.002	−0.022
bonding energy (kcal/mol)	0.52	28.17

cases two other factors play a role. First, in **T5** the β -hydrogen transfer, assisted by the Ti, increases the electron density on the Ti. Second, structure **M6**, which in fact lacks a ligand, is unsaturated, giving the phenyl group the possibility to coordinate the Ti center as much as possible (without any steric constraint), therefore resembling **M0**.

The abrupt increase in NPA charge on going from **T4** to **M5** remains so far unclear. A charge decomposition analysis (cda)¹⁹ shows an increase in amount of donation of electrons from the phenyl group from **T4** to **M5**. To use the CDA program, it was necessary for **T4** and **M5** to break the $-\text{CMe}_2-$ bridge between the phenyl group and the Cp group to obtain two separate ligands: a benzene and a Cp[−] ligand. Only the Cp group was reoptimized, whereas all other atoms were frozen. Although these final structures are not the same as **T4** and **M5**, the interaction between the phenyl group and the Ti is essentially the same (we ignored the changed influence of the Cp ligand on the Ti, which in turn affects the Ti–phenyl interaction). In fact, the only difference is the usage of a hydrogen atom instead of the bridging C atom on the phenyl group. Table 1 summarizes the most important elements of the Ti–phenyl interaction for **T4** and **M5**. From this table it becomes immediately clear that the phenyl ring is more firmly bound to the Ti center in **M5** than in **T4**, as can be seen from the large difference in bonding energies: 28.2 and 0.5 kcal/mol, respectively. Also, the amount of electron donation from the phenyl group to the Ti center is significantly larger in **M5** than in **T4**, whereas the amount of back-donation is negligible in both cases. Consequently, a higher net electron population would be expected in **M5**; however, the natural population analyses show the contrary. Therefore, Coulombic interactions are likely to play an important role as well in the overall interaction between the phenyl group and the Ti center.

(19) Dapprich, S.; Frenking, G. *J. Phys. Chem.* **1995**, *99*, 9352–9362.

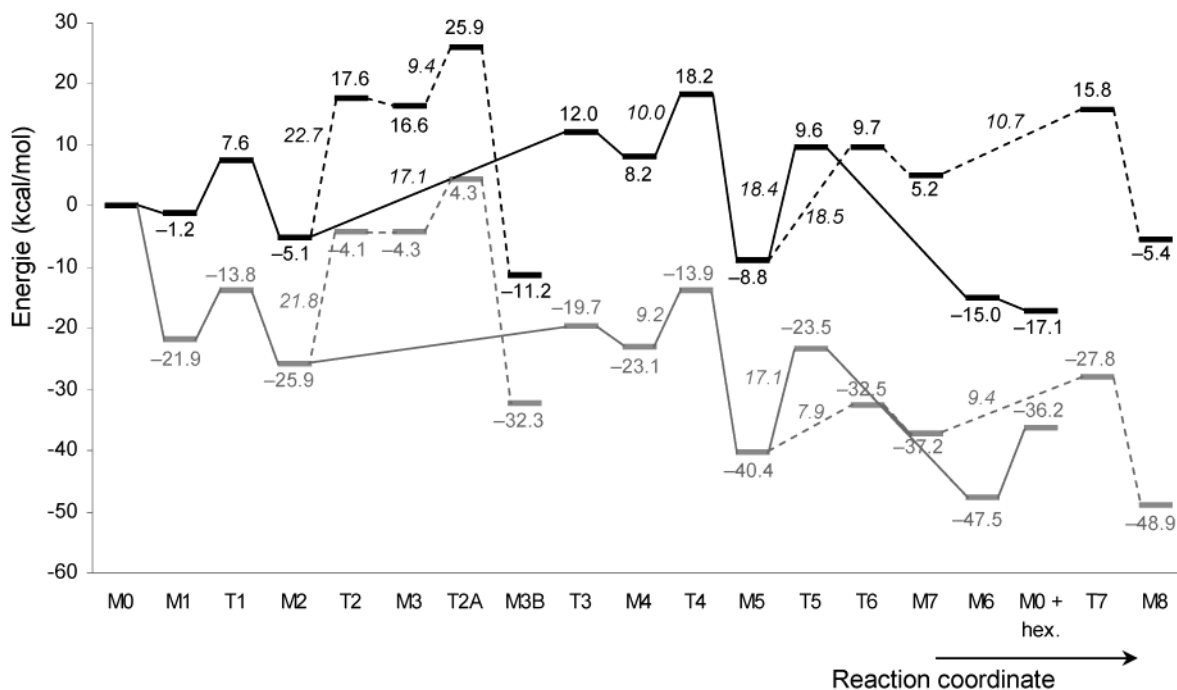


Figure 4. Schematic representation of the Gibbs free energy surface at the B3LYP/BS2 level at 298.15 K. The solid lines show the most favored pathways, whereas the dotted line shows two alternative pathways. Energy differences (kcal/mol) are expressed with respect to **M0** corrected for the corresponding number of ethylene molecules. The energy differences between two subsequent stationary points are indicated in italics. The SCF energies corrected for the ZPE contributions are plotted in gray.

Upon comparison of the structures **T2** and **T5** it is seen that the shorter Ti–H distance has a direct consequence on the NPA charge of Ti, which is considerably smaller in **T2** than in **T5**: 0.655 and 0.717 e, respectively. The higher net atomic charge on Ti in **T5** results in a stronger Ti–phenyl interaction, which could explain in turn the shorter average Ti–C_{phenyl} distance.

From a chemical point of view, the series **T6**, **M7**, **T7**, **M8**, and **M9** is the analogue of **T3**, **M4**, **T4**, **M5**, and **M6**: addition, insertion, and ring opening. From Figure 2 it also follows that these two series are very alike. Consequently, it can be concluded that on the basis of geometrical and NPA charges alone, the observed experimental selectivity cannot be explained. To do so, a detailed energetic diagram is needed to evaluate the relative stabilities of the various stationary points.

Alternatively, Figure 2 clearly demonstrates that the phenyl group shows a hemilabile character. As soon as there is sufficient place for the phenyl group, it coordinates (e.g. in **M0**, **M1**, **T1**, **M2**, **T2**, **M3**, **M5**, **T5**, **M6**, **M8**, and **M9**) and the average Ti–C_{phenyl} distances are smaller than 3.5 Å. The hemilability appears therefore to be mainly, but not exclusively, a consequence of steric constraints.

Energetic Aspects and Mechanistic Considerations. Structure **M0** has been chosen as a reference structure, and the energies of the following intermediates and products are related to **M0** corrected with the right number of ethylene molecules. In Figure 4, the variations in the Gibbs free energy and in the electronic energy corrected for the zero-point energy are both plotted for the stationary points along the reaction pathway.

The energy levels of the analogous metallacycles **M2**, **M5**, **M8**, and **M10** (the last stationary point has not

Table 2. Changes in Electronic Energy (Corrected for Gibbs Free Energy Contributions) upon Increasing the Size of the Metallacycle with One Ethylene Unit

structure	size ^a	$\Delta(\text{SCF})^b$ (kcal/mol)	$\Delta(\text{SCF} + G_{\text{corr}})^c$ (kcal/mol)
M2 → M5	5 → 7	–18.2	–3.7
M5 → M8	7 → 9	–12.7	+3.5
M8 → M10	9 → 11	–22.1	–7.0

^a Number of C atoms + Ti⁺. ^b B3LYP electronic energy. ^c B3LYP electronic energy with Gibbs free energy corrections (298.15 K).

been taken up in Figure 4) clearly demonstrate that the thermodynamic stability alone is not sufficient to explain the experimentally observed reaction selectivity.³ In Table 2, the energetic change is presented upon increase of the metallacycle by one ethylene unit. Neither the changes in electronic energy (which could be taken as a measure of the change in enthalpy) nor the changes in the Gibbs free energies show a trend that could explain the selectivity. Although the **M5** → **M8** transition is accompanied by an increase in energy by +3.5 kcal/mol, suggesting that large metallacycles are thermodynamically disfavored, this trend does not appear to be systematic. The transition **M8** → **M10** namely is again thermodynamically favored (–7.0 kcal/mol).

From this table two conclusions can be drawn (i) Inclusion of entropic effects does not alter the tendency of the stability of the increasing metallacycle; in fact, inclusion of zero-point energies and Gibbs free energy corrections shifts the energy differences by roughly 15 kcal/mol. (ii) **M8** appears to be relatively unstable. The origin of this instability might be found in the several close H–H contacts that are present in **M8** (Figure 1), which are absent in **M5** and **M2**. From these first results, it can be concluded that the changes in the

Table 3. Relative Stability of the Metallacycles with Respect to Their Corresponding Ring-Opened Structures

structure	size ^a	$\Delta(\text{SCF})^b$ (kcal/mol)	ΔG^c (kcal/mol)
M2 → M3B	4	-7.8	-6.1
M5 → M6	6	-8.3	-6.2
M8 → M9	8	-15.9	-17.1
M10 → M11	10	-14.1	-16.8

^a Number of C atoms. ^b B3LYP electronic energy. ^c B3LYP electronic energy with Gibbs free energy corrections (298.15 K).

Gibbs free energy cannot explain the observed experimental selectivity.

On the other hand, the relative stability of cycloalkanes is often calculated as the difference in energy between a cycloalkane and its corresponding *n*-alkane. This energy difference is generally considered as the strain energy due to deviation from the ideal bond angles or/and dihedral angles and the presence of close H–H contacts. This approach shows, for example, that cyclohexane is relatively the most stable cycloalkane.²⁰ A similar method was applied to the Ti metallacycles **M2**, **M5**, and **M8** to give after the ring opening products **M3B**, **M6**, and **M9**, respectively.²¹ Table 3 shows that the five- and seven-membered metallacycles are almost equally stable, as can be seen from their nearly equal strain energies: -6.1 and -6.2 kcal/mol, respectively. However, the nine-membered ring **M8** contains considerably more strain energy (-17.1 kcal/mol), which firmly suggests that this metallacycle is thermodynamically disfavored.²² However, to know whether it is formed, it is necessary to analyze the transition state leading to **M8** and its competing TS to yield the ring-opening product **M6**. Accordingly, in the next paragraphs the relative stabilities of the calculated stationary points leading to **M6** and **M8** will be discussed.

The reaction starts with the takeup of two ethylene molecules by **M0**, which is an exothermic process that releases -1.2 kcal/mol. It is interesting to note that without taking entropic effects into account, but with inclusion of ZPE corrections, the same reaction is exothermic by -21.9 kcal/mol. The formation of the σ C–C bond requires a barrier of 8.8 kcal/mol to be overcome (**T1**) to finally yield **M2**. As mentioned above, the five-membered metallacycle can already principally undergo a ring-opening reaction. On the B3LYP/BS1 potential energy surface (PES) we could locate the transition-state structure that connects **M2** and **M3**: i.e., via a reductive hydride transfer. Any attempt to locate the geometry corresponding to transition state **T2B**, involving a direct β -hydrogen transfer to give **M3B**, failed and only yielded the transition state that was already found (**T2**). We attribute the geometrical constraints, i.e. the relatively small size of the metallacycle, to the absence of this stationary point on the B3LYP/BS1 potential energy surface. The ring-opening reaction requires an activation energy of +22.7 kcal/

mol, and the reaction **M2** → **M3** itself is also highly endothermic (+21.7 kcal/mol). On the other hand, the addition of a new (third) ethylene molecule is endothermic as well. However, in this case the barrier to overcome is drastically lower (17.1 kcal/mol), and the reaction is endothermic by “only” +13.3 kcal/mol. These results strongly indicate that 1-butene will hardly be formed, which is also experimentally observed.³ It might be surprising that the addition of the third ethylene has such a high barrier. However, one has to consider that the hemilabile phenyl group has to dissociate, and also the takeup of an ethylene molecule is entropically disfavored. Calculations at the B3LYP/BS1 level without ZPE and other thermodynamic corrections taken into account²³ show that the dissociation of the phenyl group in **M2** costs about +15 kcal/mol, and the coordination energy of an ethylene molecule is also close to -15 kcal/mol. Hence, the step **M2** → **T3** involves three main contributions: (i) enthalpic effect of the decoordination of the phenyl ligand (~+15 kcal/mol), (ii) enthalpic effect of the coordination of the ethylene molecule (~-15 kcal/mol), and (iii) entropic contributions (~+13 kcal/mol).

The insertion reaction of the (third) ethylene has a moderate activation energy of 10.0 kcal/mol (**T4**), and the reaction itself is exothermic (-17.0 kcal/mol), as a result of the partial recoordination of the phenyl ligand in the obtained product **M5**. **M5** can either undergo a ring-opening reaction (via agostic assisted β -hydrogen transfer or via a hydride formation) or can continue to adsorb a new (fourth) ethylene molecule. For the two possible ring-opening reactions only the TS corresponding to the β -hydrogen transfer could be located on the B3LYP/BS1 potential energy surface. To reach this transition state structure (**T5**), a significant barrier of +18.4 kcal/mol has to be overcome. We have attempted to locate the analogue of **T2**, but for this transition state only the root-mean-square gradient convergence criterion could be met during the optimization. The maximum force criterion was practically met, indicating that we were close to a stationary point. Moreover, the energy of the(se) structure(s) was significantly higher (~10 kcal/mol) as compared to **T5**. These results demonstrate that the ring-opening reaction preferably occurs via agostic assisted hydride transfer rather than in a two-step way via a Ti–H species.

Alternatively, the reaction can proceed by the coordination of a fourth ethylene. In this case, a similar transition-state structure (**T6**) is expected for the addition to give **M7**. The reaction **M5** → **M7** is slightly more endothermic (+14.0 kcal/mol) as compared to the analogous reaction **M2** → **M4** (+13.3 kcal/mol), and the barrier for addition is somewhat higher: +18.5 and +17.1 kcal/mol, respectively.

The ethylene insertion (**M7** → **T7**) also requires a very similar barrier as compared to **M4** → **T4**: 10.6 and 10.0 kcal/mol, respectively. Interestingly, the whole insertion step is only exothermic by -10.6 kcal/mol (**M7** → **M8**), while it is -17.0 kcal/mol for **M4** → **M5**. The smaller exothermicity of the reaction **M7** → **M8** is likely due to the **M8** internal instability caused by close H–H contacts (see Figure 1).

(20) Engler, E. M.; Andose, J. D.; Schleyer, P. v. R. *J. Am. Chem. Soc.* **1973**, *95*, 8005–8025.

(21) Although the calculations do not predict the **M3B** formation, this structure has been used in order to make an analogous comparison with the higher homologues.

(22) Both **M8** and **M10** exhibit several close H–H contacts. Although a full conformational analysis on these structures is quite expensive in computational time, we have confirmed the absence of eclipsed C–C–C interactions in these structures.

(23) These kinds of corrections generally have only a minor influence on the total energy (differences).

The critical intermediates in this reaction scheme are **M2** and **M5**. The intermediate **M2** can undergo a ring-opening reaction to finally yield 1-butene. In this case a barrier of 22.7 kcal/mol needs to be overcome. On the other hand, the takeup of a new ethylene molecule requires an energy of 17.1 kcal/mol. Despite this significantly high barrier, it is substantially less than for the ring-opening reaction; therefore, our calculations predict that the reaction will continue. The insertion of another ethylene molecule demands a relatively low barrier of 10.0 kcal/mol. Once the metallocycle has grown by one ethylene unit (**M5**), the takeup of a fourth ethylene molecule is slightly less favorable than the ring-opening reaction: +18.5 vs +18.4 kcal/mol, respectively. On the basis of only these two figures practically equal Boltzmann populations can be expected for **T5** and **T6**. However, it is important to keep in mind that once the (fourth) ethylene is coordinated, there is a small gain in energy (-4.5 kcal/mol) to yield **M7** and subsequently a new barrier of 10.7 kcal/mol for the insertion step has to be overcome. Alternatively, **T5** → **M6** releases -24.6 kcal/mol. If one now considers the backward reactions, i.e., **M6** → **T5** and **M7** → **T6**, the former reaction requires a barrier of +24.6 kcal/mol, whereas the latter requires only +4.5 kcal/mol. From this it follows that the back-reaction for the reaction **M5** → **M6** can completely be ignored, whereas that of **M5** → **M7** cannot. Therefore, from a statistical point of view, the calculations show a selectivity for the formation of **M0** + 1-hexene with respect to **M8**, which is in agreement with the experimental findings. Furthermore, an increase of the temperature to 100 °C enlarges both energy barriers, but slightly more for the reaction **M5** → **T6** than for **M5** → **T5**: 21.2 and 20.3 kcal/mol, respectively. Hence, the calculations predict an increase of selectivity upon temperature increase as well a decrease in activity of the catalyst due to an augmentation of the barriers. This latter phenomenon is also experimentally observed; the productivity drops from 2787 to 440 kg of C₆/(mol of Ti) h upon going from 30 to 80 °C.³ Additionally, it should be noted that, in this temperature range, there is experimentally a decrease in selectivity due to an enhanced polyethylene formation. However, the reactions leading to polyethylene have not been explored; therefore, our study cannot give any insights into this competitive reaction.

Parallel to the theoretical study of Houk and Yu,⁷ if one combines the coordination + insertion step, since **T6** is (only) the transition of the coordination process, the barrier to overcome becomes 24.6 kcal/mol. That barrier is significantly higher than for the ring-opening reaction (18.4 kcal/mol), suggesting that mainly 1-hexene will be produced and not the higher homologues.

It can be argued that in the titanium system the **M5** → **M6** ring-opening reaction step itself requires a barrier that is relatively high.²⁴ On the other hand, the same ring-opening step in the tantalum system, which also occurs via an agostic-assisted hydride shift, requires a barrier of 25.5 kcal/mol.⁷ The large barrier in the titanium system might be due to some geometrical strain (vide supra). We have attempted to find a lower energy pathway by determining the transition state

similar to **T5**, in which an additional (fourth) ethylene was coordinated to the Ti, the coordination site previously occupied by the phenyl group. This transition state, connecting **M7** and **M6** to which an ethylene molecule is coordinated (**M6-ethylene**), has an energy that is less favorable than **T5**, i.e., $\Delta G^\ddagger(\mathbf{M7} \rightarrow \mathbf{M6-ethylene}) = 27.8$ kcal/mol, instead of $\Delta G^\ddagger(\mathbf{M5} \rightarrow \mathbf{M6}) = 18.4$ kcal/mol. Moreover, since the reaction **M7** → **M8** has a barrier of 10.7 kcal/mol, the eventually formed **M7** is preferentially transformed into **M8**, rather than into **M6-ethylene**.

In principle, the coordinated 1-hexene in **M6** could react with an ethylene molecule to give branched oligomers. The addition reaction **M6** + ethylene → **M6-ethylene** is highly endothermic. However, the exchange reaction **M6** + ethylene = **M0-ethylene** + 1-hexene is thermodynamically favored: $\Delta G = -13.2$ kcal/mol. This is mainly due to the much better coordination of the ethylene molecule to the metal center ($r(\text{Ti}-\text{C}_{\text{ethylene}}) = 2.234$ and 2.263 Å) than of the 1-hexene in **M6**: $r(\text{Ti}-\text{C}_{\text{hexene}}) = 2.383$ and 2.616 Å). Indeed, one H atom borne by the C3 atom of 1-hexene interacts repulsively with a hydrogen atom of the cyclopentadienyl group, causing the tilting of 1-hexene. Hence, once it is formed, 1-hexene will be exchanged by an ethylene molecule, as confirmed by the experimental data, with only about 3.5% of cotrimers of 1-hexene and ethene.

Importance of the Hemilabile Phenyl Ligand.

We have also investigated the effect of the pending phenyl ligand by replacing this ligand with a noncoordinating methyl ligand. According to the experimental work of Hessen et al., this ligand mainly yields polyethylene (PE). The two crucial reaction steps determining the reaction selectivity have been studied for this ligand: the ring-opening reaction (**M5** to **M6**) and the addition + insertion reaction to yield the corresponding nine-membered-ring product, i.e., **M5** to **M8**.

It can be expected that a more labile ligand is likely to destabilize **T5** (or **T2**), as result of the lacking electron donation of the ligand to the metal center, whereas species such as **M7** would be stabilized as a result of better ethylene coordination. Furthermore, **T6** would be stabilized, since the decoordination of the pending ligand becomes less costly. Such trends would predict a higher percentage of PE formation. Figure 5 compares the energy levels of these two reaction steps for both the methyl and phenyl ligands.²⁵

First, Figure 5 confirms the assumption that **M7** is more stable by 13.7 kcal/mol with a methyl than with a phenyl ligand. Second, the ring-opening reaction becomes more costly in the case of a methyl ligand. Since this reaction does not occur in a concerted way as with the phenyl ligand, but in a two-step mechanism (**M5** → **T5A** → **M6A** → **T5B** → **M6**), two barriers of identical energy (12.7 kcal/mol) need to be overcome. The overall barrier for the ring-opening reaction is 22.7 kcal/mol, which is superior to the barrier with the phenyl group (18.4 kcal/mol). More importantly, the barrier for the addition + insertion reaction (**M5** → **M8**) is only 14.3 kcal/mol. These results clearly show, when a methyl group is used, that addition + insertion reactions

(24) Margl, P.; Deng, L.; Ziegler, T. *J. Am. Chem. Soc.* **1999**, *121*, 154–162.

(25) In Figure 5, the species **M1** has been taken as a reference, since **M0** with R = methyl is very unstable because the Ti is highly unsaturated.

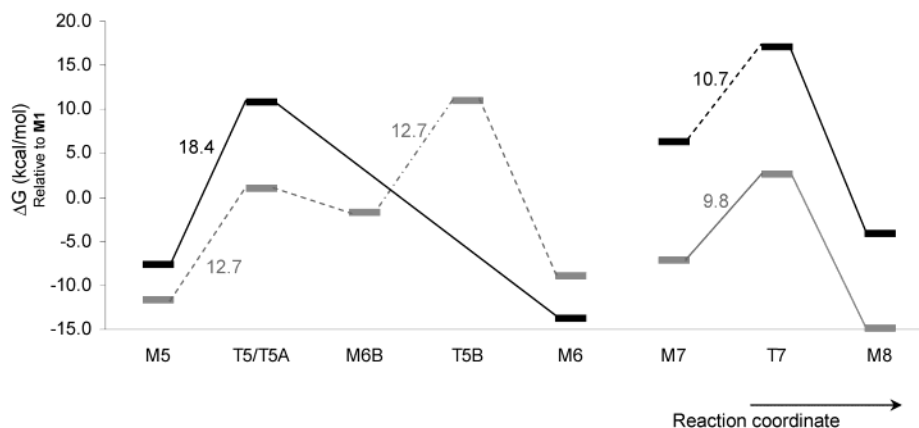


Figure 5. Schematic representation of the Gibbs free energy surface at the B3LYP/BS2 level at 298.15 K for $R = \text{phenyl}$ (in black) and $R = \text{methyl}$ (in gray). The solid lines show the most favored pathways, whereas the dotted lines show alternative, but not favored, pathways. Energy differences (kcal/mol) are expressed with respect to **M1** corrected for the corresponding number of ethylene molecules. The energy differences between two subsequent stationary points are indicated in italics.

leading to PE are more favorable than ring-opening reactions (yielding e.g. 1-hexene), which is in agreement with the experimental data. It can be added that PE could also be obtained via a different “degenerated” mechanism,²⁶ which could exhibit even smaller barriers.

Nevertheless, from a general point of view, the role of the hemilabile ligand is thus to control the number of ethylene molecules added and inserted, by successively coordinating and dissociating from the metallic center.

4. Conclusions

In light of its promising industrial perspectives, we have investigated in this computational study the trimerization reaction of ethylene that selectively yields 1-hexene with the use of such a homogeneous catalyst containing a Ti^+ , a cyclopentadienyl ligand, and a phenyl group. With the use of density functional theory (B3LYP functional) a plausible reaction scheme, containing termination reactions toward 1-butene and 1-octene, has been explored. For the final energy comparison an improved basis set was used with respect to the basis set for the geometry optimizations: cc-pVTZ (without f functions) and a 6-31G(d,p) basis set for the carbon and hydrogen elements, respectively, and a triple- ζ contraction of the Hay–Wadt pseudopotential and LanL2DZ pseudopotential for Ti, respectively.

We have shown that the ring-opening reactions are governed by geometrical constraints. If the metallacycle is sufficiently large, the intramolecular β -hydrogen transfer, assisted by Ti, occurs in a plane with the two carbon atoms. However, if the metallacycle is too small, the Ti–H interaction is larger and the C–H interactions are weaker, leading to a titanium–hydride species.

The computations, based on Gibbs free energies at 298 K, clearly show that the critical reaction barrier in forming 1-butene is substantially higher than that forming a species that leads to 1-hexene or a higher homologue. This is mainly due to geometrical constraints to open the five-membered metallacycle. In contrast, the ring-opening reaction to finally yield

1-hexene is slightly lower in energy than the coordination of a fourth ethylene molecule: 18.4 and 18.5 kcal/mol, respectively. Since the coordination reaction is a highly endothermic reaction that is directly followed by an insertion reaction with an energy barrier of 10.7 kcal/mol, while the ring-opening reaction is exothermic, our calculations predict a selectivity in 1-hexene, which is in agreement with the experimental results available.

Our work also points out the key role of the hemilability of the phenyl ligand on the final product composition. The phenyl group is indeed a pending group, as already suggested by the experimentalists.³ The hemilability of the phenyl ligand is mainly a result of steric constraints: it coordinates to the Ti^+ ion if there is sufficient room during the opening reaction steps, yet it is replaced by an ethylene molecule during ethylene addition steps. In the former case, the ligand coordination has a stabilizing effect, whereas in the latter, its decooordination induces a destabilization of the system.

Upon interchange of the phenyl group with a permanently decoordinated methyl group, the calculations show that the increase of the seven-membered metallacycle has a lower energy barrier ($\Delta G^\ddagger = 14.3$ kcal/mol for addition + insertion) than the competitive ring-opening reaction ($\Delta G_{\text{overall}}^\ddagger = 22.7$ kcal/mol). Hence, addition + insertion reactions are favored by a decoordinated ligand finally leading to polyethylene, which is the main product experimentally observed. As a consequence, in such a way we explain why the use of a hemilabile ligand yields a higher 1-hexene selectivity.

Currently, the effects of different (hemi)labile ligands are being studied for this trimerization/polymerization reaction.

Acknowledgment. We wish to thank Drs. T. Demuth, L. Saussine, and H. Olivier-Bourbigou for fruitful discussions. The Institut Français du Pétrole is greatly acknowledged for allowing the publication of these results.

Supporting Information Available: Listings of the Cartesian coordinates for all stationary points. This material is available free of charge via the Internet at <http://pubs.acs.org>.

(26) (a) Cossee, P. *J. Catal.* **1964**, *3*, 80. (b) Arlman, E. J. *J. Catal.* **1964**, *3*, 89. (c) Arlman, E. J.; Cossee, P. *J. Catal.* **1964**, *3*, 99.